Bohmian Total Potential View to Quantum Effects III. Tunnelling in Phase Space†

María F. González,‡,|| Josep Maria Bofill,§,|| and Xavier Giménez‡,||

‡ *Departament de Química Física,* § *Departament de Química Orgànica,* || *Institut de Química Teòrica i Computacional (IQTCUB), Universitat de Barcelona, Martí i Franquès 1, 08028 barcelona, Spain*

Received: June 1, 2009; Revised Manuscript Received: October 5, 2009

The tunnel effect in one-dimensional collision problems is analyzed in terms of numerical wavepacket time propagations, in position, momentum, and phase space representations of the problem. Bohm's total potential is used to provide a classical-like description of tunnelling quantum dynamics, under a time- and density-dependent potential. Wigner, Husimi, as well as Bohm phase space distributions are used in the present study, with their relative performances for the present problem having been analyzed.

I. Introduction

This work is the third of a series[1,2] devoted to the characterization of Bohm's total potential (BTP), and its use for a Bohmian, alternate interpretation of quantum effects in dynamical processes. In particular, it focuses on the use of quantum phase space distribution functions, for the computation of transmission factors in one-dimensional (1D) collision problems. The ultimate goal is a quantitative characterization of the tunnel effect, using a classical-like view of particle dynamics—under a time- and density-dependent potential energy.

The first paper of the series,[1] hereafter called Paper I, presented a method for evaluating BTP from wavepacket propagation, in terms of a simple product of matrices. The result has been the ability to compute BTP at any time increment, so as to look at its time development, as a function of the particle's initial state and the form of the classical potential. This study singled out the importance of the initial state density, since its form appeared to control the BTP shape for most of the time interval.[3] The radar wave analogy on BTP,[4,5] along with its time-dependence, prompted an additional study,[6] by which a dependence of quantum transmission on the initial launching distance, between the packet and the barrier, was inferred. This counterintuitive dependence leads, in favorable cases, to a quantitative increase in transmission the shorter is the launching distance, up to 20% per Å. The second paper,[2] Paper II, is devoted to a quantitative analysis of resonance features, in terms of BTP temporal oscillations. The oscillation amplitude is found to depend on the usual features: the barrier height and width, the well depth and width, as well as the wavepacket parameters, mainly width and central momentum. However, the oscillation frequency is solely dependent on the classical potential steepness, that is, on how fast the classical barrier height and well depth develop, as a function of position.

The present work is a continuation in the quantitative characterization of quantum phenomena, under Bohm's total potential view. As stated, Bohm's view to quantum mechanics provides a classical-like description. For instance, a tunnelling event is described as a trajectory having its energy below the classical barrier, but *above the BTP barrier at the time interval it is crossed*. Such statement is done on the basis of the classical-like structure of the defining differential equation, the quantum Hamilton−Jacobi (QHJ) equation:[4,5]

$$\frac{\partial S}{\partial t} + \frac{(\nabla S)^2}{2m} - \frac{\hbar^2}{2m}\frac{\nabla^2 R}{R} + V = 0 \tag{1a}$$

However, the exact transformation of the TD Schrödinger equation generates, in addition, a continuity equation coupled to QHJ:

$$\frac{\partial R^2}{\partial t} + \nabla\left(\frac{R^2 \nabla S}{m}\right) = 0 \tag{1b}$$

so that the analysis has to take into account both equations. Nevertheless, there exists the possibility of still focusing on just one primary equation, for both equations may combine into a single one, by means of the Theory of Characteristics.[6] The result is a unique integro-differential equation for the real quantity S, formerly the phase of the (complex) Schrödinger's wave function:

$$\begin{aligned}&\frac{\partial S(\mathbf{x},t)}{\partial t} + \frac{(\nabla_{\mathbf{x}} S(\mathbf{x},t))^T(\nabla_{\mathbf{x}} S(\mathbf{x},t))}{2m} - \\ &\frac{\hbar^2}{2m}\{\frac{1}{4m^2}[{}_C\int_{t_0}^{t}\nabla_{\mathbf{x}}(\nabla_{\mathbf{x}}^2 S(\mathbf{x},t'))\mathrm{d}t']^T \times \\ &[{}_C\int_{t_0}^{t}\nabla_{\mathbf{x}}(\nabla_{\mathbf{x}}^2 S(\mathbf{x},t'))\mathrm{d}t'] - \\ &\frac{1}{2m}{}_C\int_{t_0}^{t}\nabla_{\mathbf{x}}^2(\nabla_{\mathbf{x}}^2 S(\mathbf{x},t'))\mathrm{d}t'\} + V(\mathbf{x}) = 0\end{aligned} \tag{2}$$

This result is a structurally cumbersome equation, for which it is not straightforward to state that physical events behave classical-like. For instance, the influence of the action function depends on the history of the problem, as it appears in the third term between braces, in eq 2. This may have the meaning that the energy-spreading nature of wavepackets is included into this integro-differential equation, so that, for example, transmission might be naturally endowed with an energy uncertainty, hence allowing under-the-barrier transmission events.

Our primary goal in the present work has been checking the fundamental classical-like hypothesis of Bohmian mechanics.

† Part of the "Vincenzo Aquilanti Festschrift".

* To whom correspondence should be addressed. E-mail: xgimenez@ub.edu.

10.1021/jp905132t
Published on Web 10/20/2009

Given the difficulties associated with a formal analysis of the integro-differential eq 2, the present study is based on numerical simulations, specifically of model, simple 1D barrier systems, so as to discard any nonessential feature. Among the wealth of existing quantum phenomena, the focus here is on tunnelling.

The computation of the tunnelling transmission probability, *from classical arguments*, requires the simultaneous knowledge of the density distribution, in both position and momentum spaces, for each time instant (since the potential barrier is time-dependent). This may be (approximately) done if one knows the phase space distribution function, for the quantum time-dependent state, and it is summed in the phase space region corresponding to momentum and position ranges leading to classical transmission, for each time increment. However, as it is well-known, the interdependence between position and momentum in quantum mechanics prevents defining rigorous quantum phase space distribution functions. There exist several proposals in the literature, which satisfy part of some postulated general requirements, set to overcome this problem.[7] Among these proposals, the best-known in molecular problems are the Wigner distribution function,[8] probably the most used, and the Husimi distribution function.[9] Since, for the present case, no formal arguments give priority to any of the proposed phase distribution functions, Wigner and Husimi phase space distribution functions will be used and tested here. In addition, the Bohm distribution function,[5] arising naturally from the guiding equation for momentum, will be used and compared to the previous ones.

The structure of the remainder of the Paper is the following. Section II focuses on the theoretical tools, whereas Section III shows and discusses results corresponding to the classical-like hypothesis check. Finally, conclusions are drawn in Section IV.

II. Theory

The problem so far studied in the present work, by computational means, corresponds to a Gaussian, minimum uncertainty wavepacket, set to collide against an Eckart potential energy barrier. The wavepacket is then time-evolved numerically, the time-dependence being computed in position, momentum and phase-space representations of the problem. The latter include Wigner, Husimi, and Bohm phase-space distribution functions.

The time propagation is performed for sufficiently long times, so as to compute the transmission factor. Whereas its computation in the position and momentum representations is straightforward, just requiring the computation of the area in the transmitted region (for position), and in the positive momenta region (for momentum), calculations in phase-space have been done differently. The purpose has been to check our main hypothesis, namely that classical-like dynamics accurately describes the complete transmission processes.

Such procedure amounts to checking whether summing the density, located precisely *on* the barrier (in position), and strictly *above* the barrier (in momentum), do reproduce the accurate transmission factors, previously obtained in both position and momentum representations. It is important to emphasize that this test cannot be performed simply by integrating the long-time density located in the simultaneous positive momenta and position region, for it may hide transmission owing to an hypothetical failure of the basic QHJ assumption, namely that motion is classical under BTP.

i. Wavepacket Propagation Method, in Position and Momentum Space. The present algorithm, for the time propagation of a given initial wave function has been given elsewhere.[1,2,6] Briefly, the time-evolved wavepacket is calculated in terms of a variational basis set expansion of the type:

$$\psi(x,t) = \sum_{j=1}^{N} \phi_j(x)\langle\phi_j|\varphi_0\rangle e^{-iE_jt/\hbar} \tag{3}$$

where just one spatial dimension has been indicated. In eq 3, $\varphi_0(x)$ is the initial wavepacket, chosen to be of Gaussian, coherent-state type. In atomic units, it reads:

$$\varphi_0(x) = \left(\frac{2\gamma}{\pi}\right)^{1/4} \exp\{-\gamma(x - x_0)^2 + ip_0(x - x_0)\} \tag{4}$$

where (x_0,p_0) establishes the center of the packet, and γ is a parameter related to the Gaussian width. When the basis in eq 1, $\{\phi_j\}$, $j = 1, ..., N$ starts from a sinc discrete variable representation (DVR) original basis, the propagation algorithm transforms to matrix products:

$$\mathbf{y}(t) = \mathbf{L}^T\mathbf{tLj}_0 \tag{5}$$

where $\mathbf{y}(t)$ is the vector, of dimension N, containing the total wave function at each grid position, at time t; $\mathbf{t}$ is a diagonal matrix with diagonal elements $e^{-iE_jt/\hbar}$, $j = 1, ..., N$; $\mathbf{L}$ is the eigenvectors matrix associated to the DVR-stationary basis change; and $\mathbf{j}_0$ is the vector corresponding to the initial wavepacket (eq 4), with components corresponding to its value at each DVR grid position.

It is not difficult to obtain the momentum representation analogue of the time-propagation formula shown in eq 5. A convenient procedure is to transform the time-dependent solution in the position representation, via Fourier transform, to momentum space. The reason is that the present DVR method for wavepacket propagation provides an especially simple matrix algorithm, casting the momentum wave function at any time, in terms of the initial wavepacket in the position representation, as

$$\mathbf{y}_p(t) = \mathbf{FL}^\mathbf{T}\mathbf{tLy_0} \tag{6}$$

where $\mathbf{y}_p(t)$ is the wave function amplitude in momentum space, $\mathbf{F}$ is the Fourier transform matrix:

$$F_{mn} = \Delta x \exp(-ix_mp_n) \tag{7}$$

with Δx the grid increment, x_m the mth discrete position in DVR space, and finally p_n the nth discrete momentum in momentum space. Expression 7 arises from a simple rectangular quadrature for the space-momentum Fourier transform, especially appealing since it uses the same DVR spatial increment. The above expressions have shown their accuracy in a recent work,[10] on a space and momentum representation analyses of the Hartman effect.

ii. Computation of BTP. The computation of the quantum potential requires evaluating the density R, *as well as its second spatial derivatives*, at any time increment. An advantage of the present formulation for the wave function time propagation is that, after suitable transformations, it leads to a simple algorithm for the computation of the quantum potential (and thus the total potential) *at any time increment*, *just by doing simple matrix algebra*. It has been shown in detail in paper I how to perform such calculation, so that here it is only provided the final expression, for the sake of simplicity.

Denoting $B = \hat{A}\hat{A}$, the squared modulus of the time propagation operator, and performing the quotient in the quantum potential expression, one gets, in atomic units[1]

$$\begin{aligned} Q(x,t) &= -\frac{1}{2m}\frac{\nabla^2 R(x,t)}{R(x,t)} \\ &= \frac{1}{8m}R^{-4}\{\frac{\partial\varphi_0^*}{\partial x}B\varphi_0 + \varphi_0^* B\frac{\partial\varphi_0}{\partial x}\}^2 - \\ &-\frac{1}{4m}R^{-2}\{\frac{\partial^2\varphi_0^*}{\partial x^2}B\varphi_0 + 2\frac{\partial\varphi_0^*}{\partial x}B\frac{\partial\varphi_0}{\partial x} + \varphi_0^* B\frac{\partial^2\varphi_0}{\partial x^2}\} \end{aligned} \quad (8)$$

thus yielding the final working expression, for the computation of the quantum potential in terms of quantities obtained during the time propagation stage.

iii. Time Propagation of the Quantum Phase-Space Distribution Functions. Wigner, Husimi, and Bohm quantum distribution functions are to be evaluated, in the present work, as a function of time. We consider their evaluation, for the three cases, from the wave function as the primary quantity. This is quite often the case for the Wigner and Husimi functions, not so frequent for the Bohm case, since the latter usually focuses on the trajectory approach[11] (rather than the wave function approach) to quantum dynamics. The following paragraphs show how this can be done from our original time propagation algorithm, so that matrix algorithms are developed for the calculation of the above quantum distribution functions.

a. Wigner Distribution Function. The Wigner distribution function is given by the expression[8]

$$F^W(q,p,t) = \frac{1}{\pi\hbar}\int_{-\infty}^{\infty} e^{-2ipx/\hbar}\psi^*(q-x,t)\psi(q+x,t)dx \quad (9)$$

At this point, we may benefit from our previous algorithm for the computation of the wave function as a vector. This vector has as many components as discrete positions are included in our complete space range. Thus, it is readily obtained that the $\mathbf{F}^W$ matrix, having dimensions (*qdim*,*pdim*), being *qdim* (*pdim*) the number of discrete positions (momenta) taken in the DVR procedure, is given by

$$\mathbf{F}^W(t) = \mathbf{GM}(t) \quad (10)$$

where $\mathbf{G}$ is the time-independent matrix given by

$$G_{k,j} = \Delta x e^{-2ix_k p_j} \quad (11)$$

whereas $\mathbf{M}(t)$ contains the product of wave function amplitudes from Wigner's expression (eq 9)

$$M_{i,k}(t) = \frac{1}{4\pi^2}\psi(q_i - x_k, t)\psi^*(q_i + x_k, t) \quad (12)$$

The product between eqs 11 and 12, as explicitly written, provides the *i*th,*j*th element of the $\mathbf{F}^W$ matrix. Even though the Wigner distribution function is positive for a Gaussian wavepacket, it is known to take on negative values as time progresses.[7,12] For this reason, it is necessary to consider alternate distribution functions.

b. Husimi Distribution Function. Among several quantum phase-space distribution functions so far proposed in the literature, the Husimi distribution function occupies a distinguished position, because it belongs to a class of non-negative functions.

The Husimi distribution function is the density operator in the squeezed state representation, of which the coherent states are a particular case.[13−15] Thus, one may generate the Husimi function simply by projecting the original, Schrödinger density, onto a basis of squeezed (or coherent) states. However, we have found it much simpler to obtain the Husimi distribution from the Wigner function, since it then yields a simple matrix algorithm for such computation.

The basis for the existence of such algorithm rests on the fact that the Husimi distribution function exactly corresponds to a Gaussian smoothing of the Wigner distribution. The relevant, initial expression is[7]

$$F^H(q,p,t) = \frac{1}{\pi\hbar}\int dp' \int dq' e^{[-m\kappa(q'-q)^2/\hbar - (p'-p)^2/\hbar m\kappa]} F^W(q',p',t) \quad (13)$$

that can be written in a matrix algorithm, given by the equation,

$$\mathbf{F}^H(t) = \mathbf{DBGM}(t) \quad (14)$$

with $\mathbf{G}$ and $\mathbf{M}(t)$ given by eqs 11 and 12, respectively, and the elements of the $\mathbf{D}$ and $\mathbf{B}$ matrices are

$$D_{i,m} = \Delta p e^{[-(1/\kappa m)(p'_i - p_m)^2]} \quad (15)$$

$$B_{j,n} = \Delta q e^{[-\kappa m(q'_j - q_n)^2]} \quad (16)$$

In eqs 13, 15, and 16, m is the mass of the system, whereas κ is an arbitrary constant. Actually, the latter gives a measure of the wavepacket width. In our present case, if κ is made to coincide with γ, the initial wavepacket width for the molecular system, the squeezed state transforms to the coherent state.

c. Bohm Phase-Space Distribution Function. Even though the Husimi distribution function is non-negative, its properties still lack some of the requirements for a strictly proper distribution function. For instance, it is found that it does not satisfy the marginals, i.e. $\int \rho^H(p,q,t)dp \neq \langle q|\hat{\rho}|q\rangle$ and $\int \rho^H(p,q,t)dq \neq \langle p|\hat{\rho}|p\rangle$, where $\hat{\rho}$ is the standard density operator.[12] A quantum phase-space distribution function fulfilling such requirement, is the Madelung−de Broglie−Bohm distribution function,[5] Bohm distribution for short, which is, in addition, quite a natural choice in the present work. It is defined from its primary quantities, R and S, in the form:

$$F^B(q,p,t) = R^2(q,t)\delta(p - \nabla S(q,t)) \quad (17)$$

so that the guiding equation is incorporated inside the definition. It is possible again to derive a matrix algorithm for its computation. The corresponding expression is shown to have the form,

$$\mathbf{F}^B(t) = \mathbf{U}(t)\mathbf{V}(t) \quad (18)$$

where the elements of the $\mathbf{U}(t)$ matrix are,

$$U_{l,k}(t) = \delta(p_k - \nabla S(q_l, t)) \tag{19}$$

that is, it is 1 for momenta being numerically equal to $\nabla S(q,t)$, and zero otherwise. $\mathbf{V}(t)$ is a diagonal matrix, with elements,

$$V_{ll}(t) = \psi(q_l, t)\psi^*(q_l, t) \tag{20}$$

The wave function $\psi(q_l,t)$ in eq 20 is the standard Schrödinger wave function, computed at the discrete position q_l, at time t. On the other hand, the function $\nabla S(q_l,t)$ may be computed directly from the wave function, for instance by means of the following *scalar* expression,

$$\nabla S(q_l, t) = \frac{1}{2}\nabla \ln\left[\frac{\psi(q_l, t)}{\psi^*(q_l, t)}\right] \tag{21}$$

even though other possibilities might be available, for instance through the computation of the quantum-mechanical flux.[16]

III. Results and Discussion

As stated, calculations in the present work seek checking the classical-like hypothesis of the QHJ equations, when the dynamics is considered under BTP. Consequently, an especially simple, 1D system, has been considered, so as to discard any complexity in the transmission factor (as, for instance, the perpendicular-to-longitudinal energy transfer in higher dimensional systems).

Figure 1 shows time snapshots of the transmission across an Eckart potential barrier, in position as well as momentum space. In short, we consider collision of a wavepacket against an Eckart barrier, with the initial conditions set to correspond to a tunnelling process. In particular, the potential energy function and its specific parameters, are the following:

$$V(x) = A\frac{e^{\beta(x-x_1)}}{(1 + e^{\beta(x-x_1)})^2}$$
$$A = 200, \quad x_1 = 0, \quad \beta = 20$$

thus providing an symmetric Eckart barrier, centered at the coordinate origin. The whole set of numerical quantities is given in atomic units. Concerning the grid data, a total of 200 DVR points have been included in the calculation. This is more than enough for convergence, so that final results may be considered numerically accurate. The spatial range runs from −10 to 10, giving a distance between consecutive DVR points of 0.05. The momentum range goes from −30 to 30, leading to a momentum increment of 0.30 between consecutive discrete values.

Figure 2 provides an illustration of the basics of the present test. It shows, on one hand, the classical potential barrier height, as a function of time. Obviously, it is a constant function. In addition, this figure displays the BTP barrier height, again as a function of time. It is a non-monotonic function, leading to very low values for short times, going through a maximum for intermediate times, whereas it tends smoothly toward the classical barrier height, at large times. The shaded area illustrates the quantum-classical barrier height differences. The classical-like hypothesis linked to the QHJ equation tells that the origin of quantum effects may be attributable to the shaded area.[17] Hence, it may explain tunneling, whenever the quantum barrier

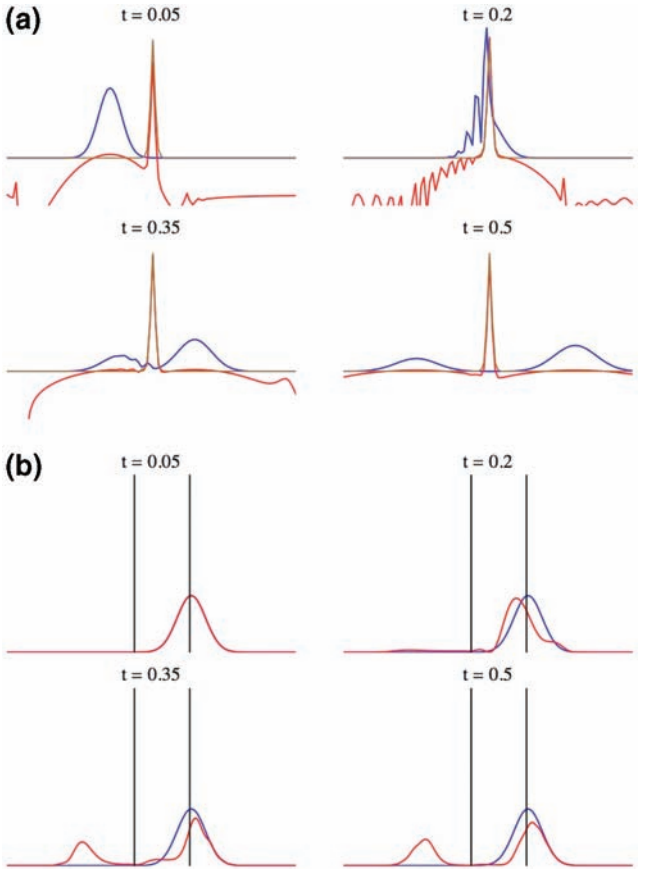

Figure 1. Time snapshots, for four different time instances (in atomic units), of a coherent state wavepacket colliding against an Eckart barrier in (a) position space, and (b) momentum space. The wavepacket initial conditions are $x_0 = -2$, $p_0 = 10$, $m = 1$, $\gamma = 1/(2\delta)^2$, $\delta = 0.4$, with being x_0 the initial location of the wavepacket center, p_0 its central momentum, m the mass, and δ the width of the Gaussian, coherent state, as given by eq 3. Panel (a): Blue trace: wavepacket density; brown trace: Eckart potential energy; red trace: BTP. Panel (b): Red trace: wavepacket density; blue trace: $t = 0$ wavepacket density, included for comparison purposes; vertical black lines: location, in momentum space, of the potential energy barrier height (rightmost line), and the zero momentum (leftmost line).

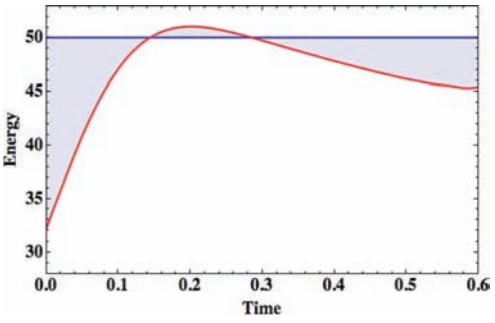

Figure 2. BTP value at the classical barrier's position, as a function of time. Blue trace: classical barrier, a constant function of time. Continuous red trace, BTP for a wavepacket with $\gamma = 0.4$.

height is lower than the classical, whereas it may lead to antitunneling when the quantum barrier is larger than the classical.

Whereas Figure 2 yields qualitative explanations for quantum effects, in terms of quantities natural to the QHJ equation, providing quantitative estimates of tunneling probabilities requires the knowledge, as a function of time, of the density distribution. However, this knowledge must be simultaneous in position and momentum, for one must be able to tell whether

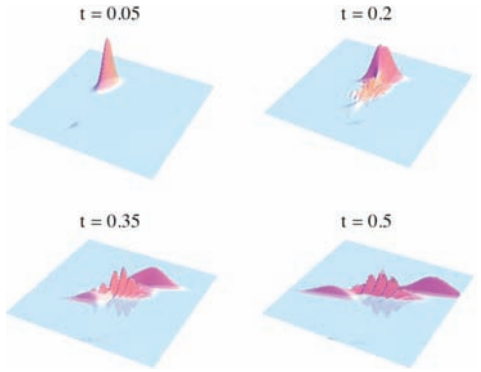

Figure 3. Time snapshots, for the same four time instances of Figure 1, of the Wigner phase-space distribution function, corresponding to the wavepacket collision against an Eckart barrier. The coordinate and momentum origin is located at the center of the *pq* plane. Note the rightwards drift of the distribution density, as time progresses, the emergence of the negative momentum part as the reflected packet is generated, along with the wiggles displaying negative values, for intermediate times.

a given density portion has enough energy to overcome a precisely located, in space, potential energy "obstacle", the potential barrier. Consequently, the quantum mechanical density has to be transformed to a phase space distribution.

Figure 3 shows the time snapshots for transmission across the Eckart potential barrier, in phase-space, using the Wigner distribution function. The plane spans the phase space coordinate ranges, whereas the vertical axis corresponds to the distribution density. The position axis runs from left to right, whereas momentum runs from bottom to top. The time-evolved distribution experiences the well-known drift toward larger positions. At a given time, the reflected part of the packet emerges as a negative momentum distribution, with positions decreasing as time increases.

It may be algebraically shown that a Gaussian wavepacket displays a Wigner distribution function which is positive everywhere.[7] However, the time-propagation and the collision against the Eckart barrier perturbs the Gaussian shape, thus making the Wigner distribution to attain an oscillating shape, leading to negative values. In particular, at intermediate times, where the largest part of the packet is on the barrier region, the Wigner function displays the highest oscillation structure, and therefore the highest negative values. As the collision further evolves, the transmitted and reflected parts recover a Gaussian-like shape, smoothing the Wigner function and leading to an essentially positive function. However, our summation procedure for the calculation of the transmission factor (see below), is strongly dominated by events occurring at intermediate times, so that the strong oscillations of the Wigner function will have an important influence.

Figure 4 shows the equivalent time snapshots of Figure 3, for the Husimi quantum phase-space distribution function. Remarkably, the Husimi function displays a smooth shape, compared to Wigner, thus reflecting what is known from the algebraic analysis of the Husimi distribution, namely that it is obtained from a Gaussian smoothing of the Wigner distribution. Consequently, the Husimi distribution is found to behave much properly than the Wigner case, mainly because it is well behaved at intermediate times, those most relevant in our summation procedure for the transmission factor.

Figure 5 displays the phase-space analogue, for the Bohm quantum phase-space distribution function. Note that this distribution is simply a 1D line on the phase-space plane, instead

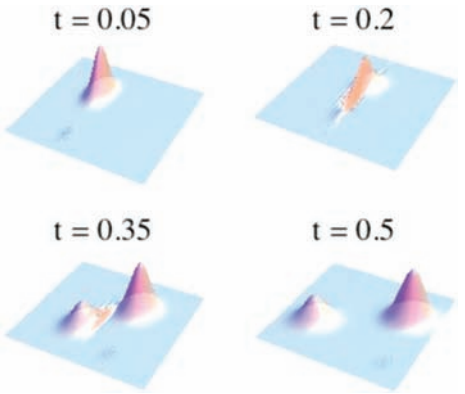

Figure 4. The same as in Figure 3, for the Husimi distribution function. Note the much smoother shape of the distribution density, compared to the Wigner case.

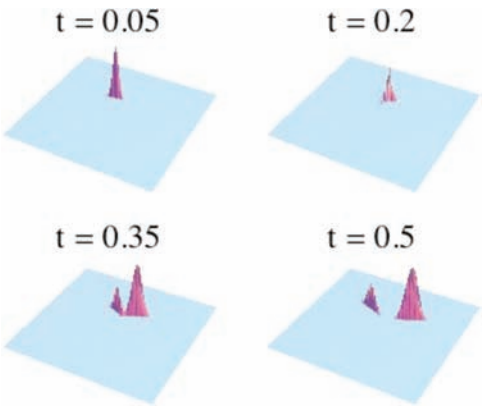

Figure 5. The same as in Figure 3 and 4, for the Bohm distribution function. The negative momentum branch, corresponding to the reflected part of the packet (as it is generated starting from the $t = 0.45$ time snapshot), displays a wrong sign, owing to a branch cut in the computation of the complex logarithm of eq 21. Fortunately, it does not affect the present work, for just the positive momentum branch is required for the computation of the instantaneous transmission.

of the solid volume of the Wigner and Husimi distributions. This is a direct consequence of the Dirac delta function appearing in the Bohm distribution function definition. In any case, however, its behavior is quite accurate, thus confirming the strong consistency of Bohm's main assumption, thus leading to the guiding equation. It has to be noted that the emergence of the negative momentum branch, corresponding to the reflected part of the packet, is contaminated by a branch cut, in the computation of the action and its gradient. Fortunately, it has no consequences to our purpose, since the computation of the transmission factor strictly focuses on the positive, transmitted part of the problem. Alternate forms for the computation of the action and its gradient, which may avoid the branch cut problem, are being currently investigated.

Having shown the time-dependent quasi-probability distributions, for the Wigner, Husimi, and Bohm cases, the information necessary for the computation of the transmission factor, under the QHJ classical-like hypothesis, is already available. The remaining work to be done is the time-sliced integration of the phase space density, simultaneously located on the potential barrier, in position space, and above the barrier, in momentum space. Figure 6 displays a diagram, which is intended to explain the basis for our time-sliced summation method, in the calculation of the transmission factor. This summation is based on the following procedure:

(1) Compute the quantum phase-space distribution function, for small time increments, from the initial state to the asymptotic

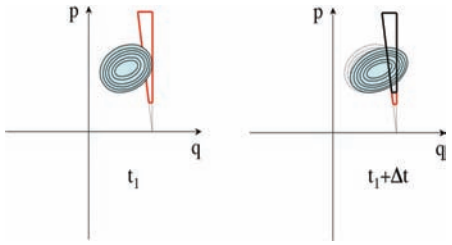

Figure 6. Schematic diagram, depicting the instantaneous integration area, used in the computation of the transmission factor, along with the contour graph, corresponding to the density distribution. The transmission factor is obtained as the sum, for all times, of the distribution density volume enclosed by that area, at each time. Note that this area is bounded by four lines, two vertical and two horizontal: the right vertical line points on BTP maximum barrier height. The left vertical line gives, for each p value, the distance Δq traveled by a phase space point in Δt, the time increment selected in our calculations to reach convergence in the present summation process. The lower horizontal line is determined by the BTP barrier height, in momentum units, at each time t and the classical barrier location. Finally, the upper horizontal line is given by the highest momentum value considered in our calculations, well above the maximum range spanned by the distribution function. The two panels correspond to two consecutive time intervals, the second panel including the information from the previous time so as to better appreciate the time evolution. The previous density distribution is shown as the dotted line, whereas the previous integration area is shown in red, the actual one being drawn in black. The area in black has its lower limit located upward, compared to the red, previous time case, since it corresponds to a typical situation whereby *Bohm's total potential barrier gets higher at the second time interval*.

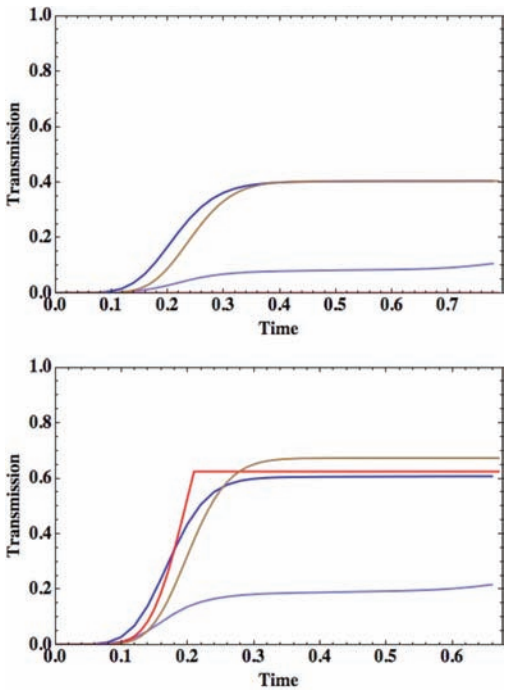

Figure 7. Cumulative transmission, as a function of time, for the accurate quantum mechanical case (brown), Wigner (light blue trace), Husimi (blue), and Bohm (red) quantum phase-space distribution functions. The complete transmission corresponds to the large time limit of the cumulative transmission. Upper panel, $p_0 = 8$, and lower panel, $p_0 = 10$ au.

stage; (2) For each time snapshot, locate in phase space Bohm's total potential barrier height; (3) Once the barrier height is located, define an integration area, for each time increment, as the capped triangle having the limits shown in Figure 6; (4) Compute the enclosed volume by the distribution density located on the area determined in 3; (5) Add this volume for each time increment. *The repeated summation for all times should provide the transmission factor, computed strictly from the density distribution located in the area of no-return, as the strict requirement for transmission in 1D classical processes*.

The results of our summation procedure are presented in Figure 7, for two representative wavepacket's initial momenta, $p_0 = 8$ and 10 au. It is observed, as expected, that transmission corresponds to the large time limit of our cumulative summation.

First, it is seen that the Wigner distribution function leads to wrong, much lower transmission factors than the accurate ones, computed from the time-dependent calculation of the transmitted area, in position space. This failure, as inspection of Figure 3 may evidence, stems from the unphysical sharp oscillations, leading to negative density values, at intermediate values of time, position, and momentum.

On the other hand, the Bohm distribution function leads to wrong predictions for low momentum, whereas it yields fairly good estimates for larger values. Actually, analysis of other initial WP conditions do show that the Bohm distribution is accurate, provided that transmission is large enough. The reasons for the low energy failure are not clear to us right now, being actively investigated in our group.

Finally, it is seen that the Husimi case gets very close to the accurate transmission value. More precisely, it is indistinguishable for $p_0 = 8$, whereas it is slightly lower for $p_0 = 10$. Interestingly, the time-dependent transmission for the Husimi case develops a bit before than the accurate one, even though the final value is accurate.

In any case, it is quite remarkable that the use of quantum phase-space distribution functions leads to such good results, when compared to accurate values. It provides confidence on their robustness in general applications, as well as on the assumptions done in the present work. In particular, it may be stated that the classical-like assumption for transmission processes is quite accurate, providing an insightful picture of deep tunneling processes. One cannot avoid describing microscopic dynamics as *a classical motion under a time-dependent, wave-like potential energy, where any tunneling process emerges from the difference between the time-dependent pattern displayed by the total potential energy and the classical potential energy*.

IV. Conclusions

The present work focused on testing the classical-like hypothesis inherent of the QHJ equation, and Bohmian mechanics in general. One-dimensional tunneling collisions of a wavepacket against a symmetric Eckart barrier have been considered, for several values of the initial collision energy.

The computation of transmission probabilities, from the classical-like QHJ hypothesis, required developing computational algorithms for the calculation of time-evolved quasi-probability distributions. In particular, formulas for such computations, in terms of a sinc-DVR propagation algorithm, have been developed and implemented, for the Wigner, Husimi, and Bohm phase-space quasi-probability functions. The use of rectangular quadratures yielded especially simple expressions, uniquely consisting of matrix products for the time propagation.

Once available the quasi-probability distributions, the actual computation of transmission probabilities required a very specific algorithm, based on calculating the density precisely on the barrier location, in position space, along with the density above the barrier height, in momentum space. Then the summation run over the whole set of time-slices, spanning the

complete transmission process. Developing such summation process required a careful testing of the numerical parameters, in particular, the time, position, and momentum increments.

Results show that the Wigner distribution is not adequate for the present purpose. The collision against the barrier generates strong oscillations in the packet, which translate into strongly negative values of the Wigner distribution, for intermediate values of time, position, and momentum. Since our summation procedure accumulates data from all times, it is not possible to get rid of such spurious oscillations by, for instance, resorting to an asymptotic analysis.

The Bohm distribution, quite natural in the present context, is shown to describe transmission under the classical QHJ hypothesis quite accurately for energies large enough, whereas it is not adequate for low energies. It is not clear right not why the Bohm distribution does not work for low energies, an hypothesis being that such distribution function may be too simple to account for a problem strongly dependent on a simultaneous spreading in position and momentum.

Finally, the Husimi distribution, a Gaussian smoothing of Wigner's, seem to work fairly well to our purpose. Results for transmission are pretty good for the energy range scanned in the present work, in some cases being indistinguishable from the exact estimation for the transmission factor.

In any case, at present it is not possible to fully state that the classical-like QHJ hypothesis has been proven to hold. First, we performed a first numerical analysis of the problem, thus being far from general. Second, we had to resort to several quasi-probability distribution functions, since it is well-known that none of them are totally rigorous. One may then argue that claiming the present test as successful, in this regard, has the distribution function as an "adjusting parameter". Consequently, a sensible conclusion here might be that a necessary, but not sufficient condition, for the classical QHJ hypothesis to hold, has been found. In other words, the computation of tunneling transmission was found sufficiently close the accurate value, for one fairly good distribution function, and a sufficiently general 1D collision problem.

Acknowledgment. It is a pleasure to dedicate this paper to Professor Vincenzo Aquilanti. One of us (X.G.) spent uncountable hours, during his thesis and postdoc days, enjoying Enzo's complete knowledge of molecular science and immense humanistic culture. Those Perugia days are among his best personal memories. In addition, our first encounter with Bohm's mechanics was provided by a research seminar delivered by Enzo, in particular on Calogero's work, and its connection to the variable phase approach to quantum dynamics. Financial support from the Spanish *Ministerio de Ciencia y Tecnología*, DGI projects CTQ2005-01117/BQU and CTQ2008-02856 and, in part from the *Generalitat de Catalunya* projects 2005SGR-00111 and 2005SGR-00175 is fully acknowledged. M.F. González gratefully thanks to Ministerio de Ciencia y Tecnología for a predoctoral fellowship.

References and Notes

(1) González, J.; Bofill, J. M.; Giménez, X. *J. Chem. Phys.* **2004**, *120*, 10961.
(2) González, M. F.; Aguilar-Mogas, A.; González, J.; Crehuet, R.; Anglada, J. M.; Bofill, J. M.; Giménez, X. *Theor. Chem. Acc.* **2009**, *123*, 51.
(3) González, J.; González, M. F.; Bofill, J. M.; Giménez, X. *J. Mol. Struct. (THEOCHEM)* **2005**, *727*, 205.
(4) Bohm, D.; Hiley, B. *The Undivided Universe*; Routledge and Kegan Paul: London, 1993.
(5) Holland, P. R. *The Quantum Theory of Motion*; Cambridge University Press: Cambridge, 1993.
(6) González, M. F.; González, J.; Bofill, J. M.; Giménez, X. *J. Math. Chem.* **2007**, *43*, 350.
(7) Lee, H.-W. *Phys. Rep.* **1995**, *259*, 147.
(8) Wigner, E. P. *Phys. Rev.* **1932**, *40*, 749.
(9) Husimi, K. *Prog. Phys. Math. Soc. Japan* **1940**, *22*, 264.
(10) González, M. F.; Bofill, J. M.; Giménez, X.; Borondo, F. *Phys. Rev. A* **2008**, *78*, 032102.
(11) Wyatt, R. E. *Quantum Dynamics with Trajectories*; Springer: New York, 2005.
(12) Hillery, M.; O'Connel, R. F.; Scully, M. O.; Wigner, E. P. *Phys. Rep.* **1984**, *106*, 121.
(13) Glauber, R. J. *Phys. Rev.* **1963**, *130*, 2529. (1963) *131*, 2766.
(14) Sudarshan, E. C. G. *Phys. Rev. Lett.* **1963**, *10*, 277.
(15) Stoler, D. *Phys. Rev. D* **1970**, *1*, 3217.
(16) González, M. F.; González, J.; Giménez, X.; Bofill, J. M. *J. Phys. Chem. A* **2007**, *111*, 10226.
(17) It is of course just one way to state the problem, which may be considered as complementary to the celebrated "energy boost" introduced by Lopreore & Wyatt: Lopreore, C. L.; Wyatt, R. E. *Phys. Rev. Lett.* **1999**, *82*, 5190.

JP905132T